Undulation Instabilities in the Meniscus of Smectic Membranes

J. C. Loudet,[1] P. V. Dolganov,[2] P. Patrício,[3,4] H. Saadaoui,[1] and P. Cluzeau[1]

[1]*Université Bordeaux 1, CNRS, Centre de Recherche Paul Pascal, Avenue A. Schweitzer F-33600 Pessac, France*
[2]*Institute of Solid State Physics, Russian Academy of Sciences, Moscow Region 142432 Chernogolovka, Russia*
[3]*Centro de Física Teórica e Computacional, Universidade de Lisboa, Avenida Professor Gama Pinto 2, P-1649-003 Lisboa Codex, Portugal*
[4]*Instituto Superior de Engenharia de Lisboa, Rua Conselheiro Emídio Navarro 1, P-1959-007 Lisboa, Portugal*

(Received 27 November 2010; published 18 March 2011)

Using optical microscopy, phase shifting interferometry, and atomic force microscopy, we characterize the undulated structures which appear in the meniscus of freestanding ferroelectric smectic-C^* films. We demonstrate that these periodic structures correspond to undulations of the smectic-air interface. The resulting striped pattern disappears in the untilted smectic-*A* phase. The modulation amplitude and wavelength of the instability both depend on meniscus thickness. We study the temperature evolution and propose a model that qualitatively accounts for the observations.

DOI: 10.1103/PhysRevLett.106.117802 PACS numbers: 61.30.Jf, 61.30.Gd, 61.30.Hn

When in contact with a solid substrate, isotropic liquids form a meniscus whose properties are controlled by the well-established laws of capillarity and gravity [1]. Wetting of liquids on surfaces, for example, is of ubiquitous importance in many industrial fields and our everyday life. The case of complex liquids, such as liquid crystals (LC), is much more complicated because of the partial ordering of molecules which imparts elastic properties.

Since the 1970s, and the discovery of the wonderful properties of LC for display devices, an incredibly large number of studies have been devoted to the wetting properties of LC in contact with solid substrates. The more specific case of smectic freestanding films (FSF) (Fig. 1), or smectic membranes, was addressed more recently [2–4]. In contrast to isotropic liquids, where the meniscus profile is exponential (e.g., soap films), the meniscus in smectic-*A* (sm*A*) FSF has a circular profile and forms a finite angle with the film (Fig. 1). The meniscus shape determines the film disjoining pressure [5], which governs its stability and is essential in many interesting phenomena, such as thinning transitions [6].

The situation is more complex in smectic-*C* (sm*C*) or chiral smectic-C^* (smC^*) phases [5,7] where the molecules are tilted with respect to the layer normal. Projection of the molecular axes onto the layer plane, defined as the **c** director, can vary in orientation and form modulated structures. Meyer and Pershan [8] described the so-called splay domains in the meniscus of sm*C* films, which were associated with surface-induced spontaneous polarization resulting in **c**-director splay. Layer undulation was proposed as a reason for the observed patterns around solid inclusions in sm*A* films [9]. Quite recently, Harth and Stannarius [10] reported studies of modulated striped structures in menisci at the film edge and around inclusions embedded in films. They interpreted the observed structures as **c**-director distortions, consistent with splay domains.

In this Letter, we focus on the meniscus of FSF and experimentally demonstrate, through a combination of techniques, that the aforementioned stripes are in fact related to undulations of the smectic-air interface. Those undulations can explain the previously reported **c**-director splay domains and they are also closely reminiscent of the universal cascade of wrinkles observed recently in various materials under strain [11,12]. A model, based on dilation-induced strain applied to the smectic layers at the sm*A*-sm*C* phase transition, is shown to be consistent with the experimental results.

We used a variety of experimental methods, namely, polarized light microscopy, phase shifting interferometry (PSI), and atomic force microscopy (AFM). Experiments were performed on several compounds, including ferroelectric materials ZLI-3488 [13], SCE-9, and SCE-12 (Merck, England). Films in the smC^* and sm*A* phases were prepared on a hole in a thin glass plate (Fig. 1). After preparation, the films were kept at constant temperature for several hours to ensure the relaxation of the meniscus shape.

Figure 2 shows the characteristic patterns in the film meniscus. The meniscus thickness increases from left to right. In the SmC^* phase, various modulated structures develop only in the meniscus and not in the film [Fig. 2(a)]. First, a 1D pattern made of a system of branched and then parallel stripes is formed. As thickness increases, a secondary modulation develops along the film

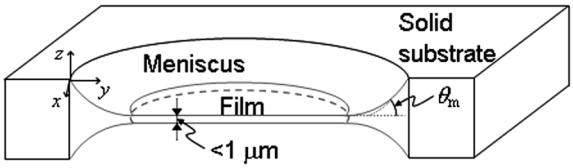

FIG. 1. Geometry of freely suspended smectic films.

thickness gradient [inset of Fig. 2(b)] and yields to the formation of a 2D pattern made of rows of squarelike domains. The period of the stripes and the size of the squares increase with meniscus thickness. As already thoroughly described in [10], the meniscus texture is independent of the chiral nature of the considered compounds but varies strongly with temperature. In freestanding films, the smC^* structure can exist above the bulk smC^*-sm$A$ transition temperature, T_C, due to surface ordering [5]. On heating close to T_C (Fig. 2), the contrast of the stripe pattern decreases gradually. Just above T_C, residual stripes remain in the meniscus [Fig. 2(c)]. They eventually disappear completely upon further heating while the square pattern partially remains [Fig. 2(d)]. The 2D pattern fades away in a stepwise manner: the squares disappear row by row, following an unzippinglike mechanism, starting from the thinner regions. Well above T_C, square domains are no longer present and the whole meniscus becomes defect-free.

On cooling back to the smC^* phase, the same patterns reappear in reverse order and so forth over heating and cooling cycles. At constant temperature, all the above structures survive for many days as long as the film is stable, in contrast to instabilities observed in sandwiched cells [5]. Note that the observed 1D and 2D patterns share some degree of resemblance with other modulated structures encountered in frustrated smectics deposited on or sandwiched between solid substrates [14].

To clarify the nature of the observed structures, we used PSI to probe the smectic-air meniscus profile, $z = u(x, y)$, with a resolution of a few nanometers. The principles of PSI and the experimental setup were described elsewhere [15,16].

Figure 3(a) shows an interferogram of a smC^* meniscus. The main feature of this image is that interference fringes are not straight but wavy in the stripes area. Therefore, the meniscus is not smooth (as in sm$A$) but rather undulated in this area. The corresponding height profile $u(x, y)$, reconstructed from a series of interferograms, is presented in Fig. 3(b). In this figure, the meniscus rises about $\simeq 8$ μm above the flat film over a distance of ~ 50 μm. The oblique dashed line in Fig. 3(b) marks the location of the broadest wrinkles seen in the inset of Fig. 3(a) while the bottom graph exhibits the associated profile. In this region, undulations occur with amplitude around $\sim$40–50 nm and wavelength $\lambda \sim 5$ μm. The existence of wavelike fringes is directly correlated to the presence of stripes: on heating above T_C, as the stripes disappear, the fringes smoothen and become straight. Close to the flat film region, the fringes turn to wavelets with smaller amplitude and wavelength. In this area, the amplitude of the wrinkles cannot be resolved as it falls within our experimental accuracy (~ 5 nm). In the thick part of the meniscus, preliminary

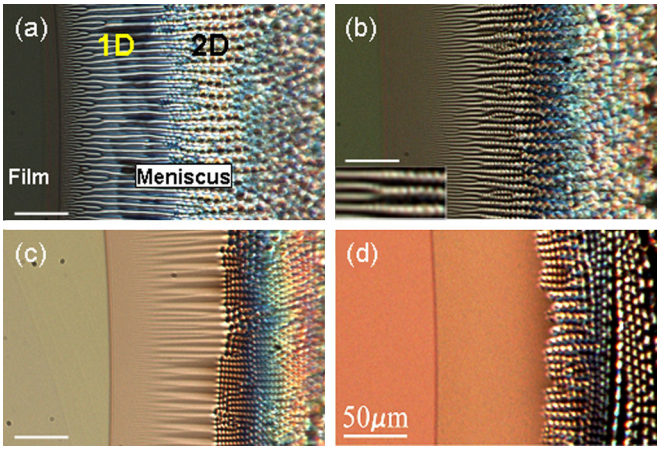

FIG. 2 (color online). Optical photographs showing the evolution of the meniscus structure with temperature (SCE-9 and SCE-12 compounds). (a) smC^* phase, $T = 37.5\,^\circ$C. 1D (2D) refers to the 1D (2D) pattern (see text). (b) $T = 67\,^\circ$C, still in the smC^* phase. Inset: Enlarged view of the region where the 2D modulation starts to appear. (c) $T = 70\,^\circ$C, just above the bulk smC^*-sm$A$ phase transition. (d) $T = 74.5\,^\circ$C, deep in the sm$A$ phase. All the photographs were taken in transmitted light with decrossed polarizers and various decrossing angles to enhance contrast.

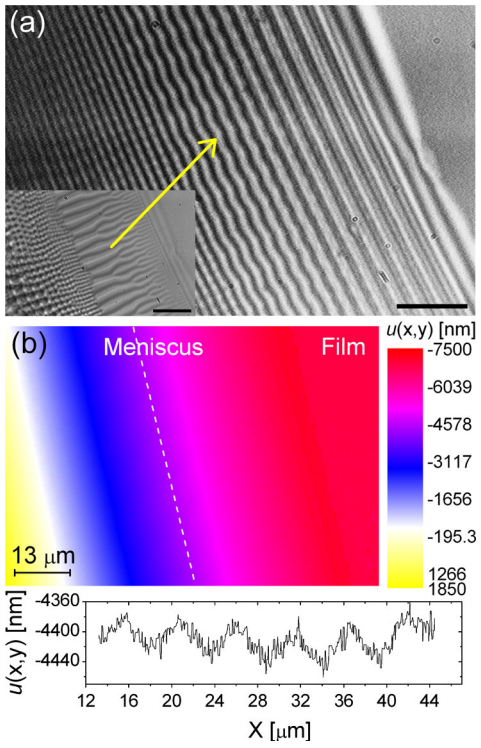

FIG. 3 (color online). (a) Interferogram of a ZLI-3488 smC^* film (reflection mode). $T = 40\,^\circ$C, scale bar: 13 μm. Inset: Corresponding optical photograph in transmitted white light. Scale bar: 16.2 μm. The arrow indicates the location of broad wrinkles in the interferogram. (b) Associated color-coded image plot of $u(x, y)$. The bottom graph shows the undulated meniscus profile along the oblique dashed line (region of broad stripes).

PSI analyses of the 2D squarelike lattice reveal that the interface undulates in two orthogonal directions. A detailed analysis of these data will be given elsewhere.

To confirm the results obtained through optical studies, we used AFM (Nanoscope Icon, Veeco, CA) to probe the meniscus structure. To our knowledge, we report here on the first AFM experiments performed on FSF. Those very delicate measurements were performed in air in the smC^* phase with the microscope operated in both tapping and peak force modes using two different tips [17]. Figure 4 exhibits the AFM results in the stripes region. The obtained image [Fig. 4(a)] and profiles [Fig. 4(b)] undoubtedly confirm the undulation of the smectic-air interface. Both the undulation amplitude ($h^{\mathrm{AFM}} \simeq 50$–$100$ nm) and wavelength ($\lambda^{\mathrm{AFM}} \simeq 8$–$10$ μm) decrease from the thick to the thin areas and are quite consistent with those inferred from PSI. Furthermore, we have checked that the stripe period deduced from the AFM profiles is equal to that derived from the *in situ* optical image recorded just before scanning the free surface. Note that the secondary undulations along the stripes in the AFM image do not represent actual interface undulations but originate from scanning artifacts.

A possible mechanism that accounts for wrinkles in smC^* menisci may be derived from the one first proposed by Johnson and Saupe [18]. Assuming a constant layer number, sm$A$ layers tend to contract upon cooling into the smC^* phase because of an increase of the tilt angle. This contraction is constrained by the strong anchoring conditions of the LC material at the ring border. The resulting mechanical stress induces a dilation which then triggers undulation of the layers. It is indeed well known that dilation-induced strain in smectics can be relaxed by layer undulations in cases of strong anchoring [5,18–21]. Like the chevron instability in ferroelectric smectics [22,23], the layers adjust their periodicity as a function of external constraints. This undulation instability may explain the existence of director splay domains without invoking surface-induced spontaneous polarization, as proposed earlier [8,10].

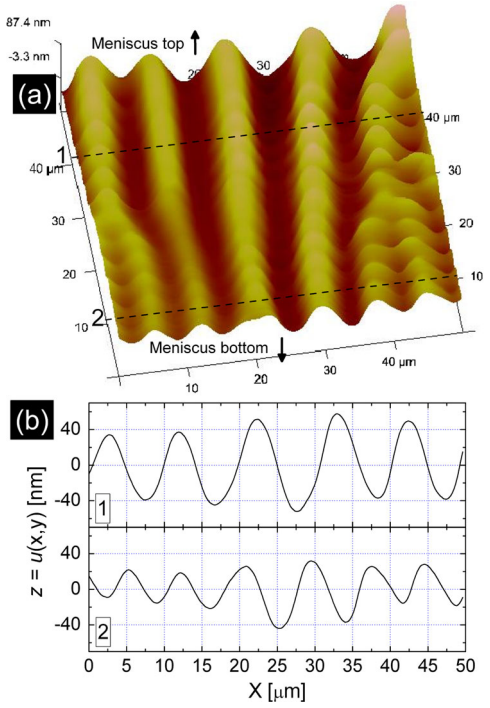

FIG. 4 (color online). (a) AFM image of the meniscus of a smC^* film in the stripes region (SCE-12 sample, $T = 20\,^{\circ}$C). The undulated profile clearly confirms PSI measurements. (b) z profiles at locations marked 1 and 2 in (a).

The anchoring conditions alone are unlikely to be responsible for the instability. In the sm$A$ phase, the molecules are anchored homeotropically at the free surfaces of the meniscus and are therefore tilted with respect to each other. Yet, no undulation appears in the sm$A$ phase. In the sm$C$ phase, such anchoring should not lead to undulations because of the additional possibility to rotate the molecules ($\mathbf{c}$ director) within the sm$C$ layers.

We can account for interfacial undulations by adding a surface tension term in the original model of Clark and Meyer [20]. Close to T_C, i.e., close to the instability threshold, we may assume a very small tilt angle and therefore use the elastic free energy of a sm$A$ liquid crystal, as a first approximation. Ignoring thickness gradients and assuming small interfacial slopes, the simplest free energy density f, in terms of the layer displacement $u(x, z)$ in the z direction, takes the form (in two dimensions)

$$f = \frac{\bar{B}}{2d\lambda}\int_{-d/2}^{d/2} dz \int_0^{\lambda} dx \left\{\left[\frac{\partial u}{\partial z} - \frac{1}{2}\left(\frac{\partial u}{\partial x}\right)^2\right]^2 + \Lambda^2\left(\frac{\partial^2 u}{\partial x^2}\right)^2\right\} + \frac{\sigma}{d\lambda}\int_0^{\lambda} dx h_x^2, \quad (1)$$

where d is the film thickness, $q_x = 2\pi/\lambda$ is the wave vector of the instability (in the x direction), $\Lambda = \sqrt{K_u/\bar{B}}$, and $h = u|_{z=d/2,-d/2}$. The first integral in f is the usual elastic contribution describing changes in layer thickness (described by the compression modulus $\bar{B}$) and splay curvature (quantified by the splay elastic constant K_u). The second integral is the additional surface tension term (σ is the smectic-air interfacial tension) which will quantify the surface energy cost associated with interfacial deformations. At the instability threshold, we may look for a solution u of the form $u(x, z) = \gamma_0 z + g(z)\cos q_x x$, where $\gamma_0 = \delta/d$ is the strain induced to the layers due to the change $d \rightarrow d + \delta$. Minimization of f with the above form of u leads to an equation for g from which we get $g(z) = g_0 \cos^{-1}(q_z d/2)\cos q_z z$, where the symmetry $g(z) = g(-z)$ and the condition $g(z)|_{z=d/2,-d/2} = g_0$ were used. $q_z = q_x\sqrt{\gamma_0 - \Lambda^2 q_x^2}$. Here, q_z is not a mere constant, as in [20], because the layers are free to undulate at free surfaces. Injecting the final field u in f, the condition for instability, $\partial f/\partial(g_0^2) \leq 0$, is met for γ_0 exceeding a threshold

$$\gamma_0 = \Lambda^2 q_x^2 + \frac{q_z d}{\alpha} \cot\left(\frac{q_z d}{2}\right), \quad (2)$$

with α a dimensionless parameter given by $\alpha = d\bar{B}/\sigma$. Because q_z is a function of q_x and γ_0, the critical wave vector q_c and critical strain γ_{0c} cannot be easily determined analytically but can be found numerically by minimizing γ_0. Taking $K_u = 10^{-11}$ N and $\bar{B} = 10^7$ J/m^3 gives $\Lambda = 10^{-9}$ m, and we estimate $\sigma \simeq 2.10^{-2}$ J/m^2 [3,24]. For a given d, the value of γ_0 is adjusted till Eq. (2) is satisfied for an appropriate q_x range. Since this model is approximate, we only look for a qualitative agreement with experiments in terms of orders of magnitude. For $d = 10$ μm, for example, this calculation predicts $\lambda_c = 0.85$ μm and $\gamma_{0c} = 3.9 \times 10^{-4}$ at threshold, corresponding to a critical displacement $\delta_c = 3.9$ nm. The computed value of λ_c is close to the experimental one derived at threshold, $\lambda_c^{\text{exp}} \simeq 1.5$–$2$ μm. Furthermore, the model predicts that λ_c increases with d, which is in line with the experimental trend in Fig. 2 and that reported in [10] (a fit of the numerical results actually reveals a precise scaling law: $\lambda_c \propto \sqrt{d}$). The dilation is greater in thicker parts of the meniscus because more layers are involved. Therefore, a dilation gradient occurs in the meniscus, suggesting that the 2D square lattice develops only when a high enough dilative strain has been reached [25]. It is then very tempting to think that this lattice corresponds to a network of focal conic domains mentioned in earlier studies [3,5,21,26] and more recently in sm*A* films deposited on crystalline surfaces [14]. Parabolic focal conic defects in particular [21] are known to nucleate in (highly) dilated sm*A* samples to (partly) relax the stress. This is what seems to occur here in the meniscus.

In the flat film region, layers are free to contract below T_C because of the two unconstrained free surfaces. No dilation (and therefore no instability) occurs there, at least within our experimental conditions (i.e., for $d \leq 1$ μm). Besides, it is well known that smectic layers can sustain compression without undulating [5]. Note, however, that Gorecka *et al.* [27] observed instabilities in FSF but only for thick enough films ($d \geq 5$ μm).

To conclude, our results provide clear-cut evidences that the meniscus structure in smC^* (sm$C$) samples is more complex than that presumed earlier as it is characterized by undulations of the smectic layers. This is the central result of this work which shows that the meniscus of a complex fluid is not always smooth but can be rough or structured. Follow-up experimental work will focus on investigating the influence of film thickness and nature of solid substrate. On the theory side, a more sophisticated model involving thickness gradients and the coupling of **c**-director distortions to layer undulations should be worked out.

The authors cordially acknowledge L. Lejček and B. Pouligny for very helpful discussions and thank J. P. Salvetat for suggesting the AFM experiments.

[1] J. S. Rowlinson and B. Widom, *Molecular Theory of Capillarity* (Dover, New York, 2002).
[2] P. Pieranski *et al.*, Physica (Amsterdam) **194A**, 364 (1993).
[3] F. Picano, R. Holyst, and P. Oswald, Phys. Rev. E **62**, 3747 (2000).
[4] A. Poniewierski, P. Oswald, and R. Holyst, Langmuir **18**, 1511 (2002).
[5] P. Oswald and P. Pieranski, *Smectic and Columnar Liquid Crystals* (Taylor & Francis, Boca Raton, FL, 2005).
[6] T. Stoebe, P. Mach, and C. C. Huang, Phys. Rev. Lett. **73**, 1384 (1994).
[7] P. G. de Gennes and J. Prost, *The Physics of Liquid Crystals* (Clarendon, Oxford, 1993).
[8] R. B. Meyer and P. S. Pershan, Solid State Commun. **13**, 989 (1973).
[9] M. Conradi, P. Ziherl, A. Šarlah, and I. Muševič, Eur. Phys. J. E **20**, 231 (2006).
[10] K. Harth and R. Stannarius, Eur. Phys. J. E **28**, 265 (2009).
[11] J. Huang *et al.*, Science **317**, 650 (2007); J. Huang *et al.*, Phys. Rev. Lett. **105**, 038302 (2010).
[12] H. Vandeparre *et al.*, Soft Matter **6**, 5751 (2010); H. Vandeparre *et al.*, arXiv:1012.4325v1.
[13] J. R. Lalanne *et al.*, Phys. Rev. A **44**, 6632 (1991).
[14] B. Zappone and E. Lacaze, Phys. Rev. E **78**, 061704 (2008), and references therein; J. P. Michel *et al.*, Phys. Rev. E **70**, 011709 (2004).
[15] J. C. Loudet, A. G. Yodh, and B. Pouligny, Phys. Rev. Lett. **97**, 018304 (2006).
[16] A. Harasaki, J. Schmitt, and J. C. Wyant, Appl. Opt. **39**, 2107 (2000).
[17] In the tapping mode, phase images were obtained using a silicon tip (stiffness $k \simeq 10$ N/m, tip radius <10 nm, $\nu = 150$ kHz) whereas Si_3N_4 tips (stiffness $k \simeq 0.4$ N/m, tip radius <10 nm) were used for imaging in the peak force mode.
[18] D. Johnson and A. Saupe, Phys. Rev. A **15**, 2079 (1977).
[19] M. Delaye, R. Ribotta, and G. Durand, Phys. Lett. **44A**, 139 (1973).
[20] N. A. Clark and R. B. Meyer, Appl. Phys. Lett. **22**, 493 (1973).
[21] C. S. Rosenblatt, R. Pindak, N. A. Clark, and R. B. Meyer, J. Phys. (Paris) **38**, 1105 (1977).
[22] T. P. Rieker *et al.*, Phys. Rev. Lett. **59**, 2658 (1987).
[23] P. Cluzeau *et al.*, Eur. Phys. J. B **3**, 73 (1998).
[24] M. Veum *et al.*, Phys. Rev. E **74**, 011703 (2006).
[25] K. Harth and R. Stannarius (private communication).
[26] J. M. Delrieu, J. Chem. Phys. **60**, 1081 (1974).
[27] E. Gorecka, M. Glogarová, L. Lejček, and H. Sverenyák, Phys. Rev. Lett. **75**, 4047 (1995).